

# Theoretical analysis of backscattered polarization patterns of turbid media containing glucose

Lanqing Xu (徐兰青), Hui Li (李 晖), and Shusen Xie (谢树森)

Key Laboratory of Optoelectronic Science and Technology for Medicine (Fujian Normal University), Ministry of Education, School of Physics and Optoelectronics Technology, Fujian Normal University, Fuzhou 350007

Received September 27, 2006

Single scattering model and Stokes-Mueller formalism are introduced to investigate the influence of glucose on backscattered polarization patterns in turbid media. Glucose molecules rotate the polarization plane and induce changes in backscattered Mueller matrix patterns. Some Mueller matrix elements present higher optical rotation as the concentration of glucose augments. Using image subtraction and integration, linear relationship between low glucose concentration in the physiological range and optical rotation degree can be derived.

OCIS codes: 170.0170, 170.1470, 260.5430, 290.7050.

Several recent studies have demonstrated that relevant information of turbid media can be derived by analyzing the Mueller matrix patterns of the diffusely backscattered polarized light<sup>[1–6]</sup>. Optical approaches including polarized means to studying turbid media with chiral components have also attracted significant interest because of the potential use in noninvasive glucose monitoring for diabetes patients<sup>[7–9]</sup>. For polarized light, glucose molecules rotate the polarization plane hence affect the propagation rules of light which can be observed in the backscattered Mueller matrix patterns. This letter concentrates on 4 special Mueller matrix elements and discusses their specificities at the presence of glucose.

Many previous works suggested that the main contribution to effective Mueller matrix came from those weakly scattered photons and the features of single scattering matrix can be preserved in the diffusely backscattered Mueller matrix<sup>[4–7]</sup>. In this letter, we use single scattering model and Stokes-Mueller formalism to deduce backscattered Mueller matrix elements, apply rotation matrix to describe glucose effect, introduce Fresnel matrix to characterize boundary effect, and define formulas for image subtraction and integration to analyze glucose-induced optical rotation for different concentrations.

We assume here that light is scattered by spheres and Mie theory can be applied. The incoming narrow beam of incoherent light propagates downward along  $z$  axis into a semi-infinite media. Let  $S_i$  be the Stokes vector of incident beam with respect to the laboratory coordinate system  $(x, y, z)$ , the differential power arriving at depth  $z$  is scattered from the differential volume  $dsdz$  into solid angle  $d\omega$ , and finally reaches the detector at point  $(\rho, \phi)$  on the upper surface of the turbid media, as shown in Fig. 1. The Stokes vector  $dS^{bs}$  corresponding to the radiance at the detector is

$$dS^{bs}(\rho, \phi) = \mu_s \frac{1}{r^2} \exp(-\mu_t(z+r)) R(\phi) F_t \times R(\alpha_2) M(\theta) R(\phi) R(\alpha_1) S_i dz, \quad (1)$$

where  $r = \sqrt{\rho^2 + z^2}$ ;  $\mu_t$  and  $\mu_s$  are the extinction coefficient and scattering coefficient, respectively;  $M(\theta)$

is the scattering matrix derived from Mie theory<sup>[10]</sup>,  $\theta = \pi - \arctan(\rho/z)$ ;  $R(\alpha_1)$  and  $R(\alpha_2)$  are Mueller matrices representing the contribution of glucose to a certain optical path,  $\alpha_i = k \times l \times c_g$ ,  $k$ ,  $l$ , and  $c_g$  are optical rotation degree, propagation path length, and glucose concentration respectively;  $R(\theta)$  is the rotation matrix connecting Stokes vectors of reference plane and scattering plane;  $F_t$  is the Fresnel matrix that describes the refraction at the boundary<sup>[11]</sup>. Backscattered Stokes vector  $S^{bs}$  of the total radiance at the detector can be obtained by integration of Eq. (1) over  $z$ ,

$$S^{bs}(\rho, \phi) = \int dS^{bs} = \mu_s \int_0^{+\infty} \frac{1}{r^2} \exp(-\mu_t(z+r)) \times R(\phi) F_t R(\alpha_2) M(\theta) R(\phi) R(\alpha_1) S_i dz. \quad (2)$$

And the backscattered Mueller matrix is given by

$$M(\rho, \phi) = \mu_s \int_0^{+\infty} \frac{1}{r^2} \exp(-\mu_t(z+r)) \times R(\phi) F_t R(\alpha_2) M(\theta) R(\phi) R(\alpha_1) dz. \quad (3)$$

The 16 elements of Mueller matrix denote different polarized properties of turbid media. For example,  $M_{11}$

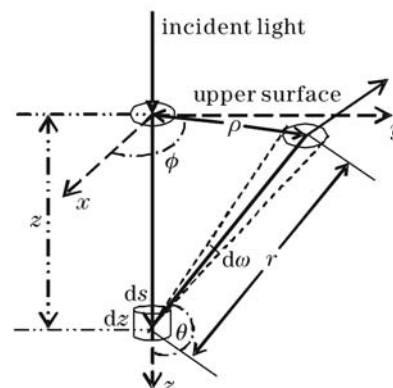


Fig. 1. Single scattering geometry.

represents the intensity transformation of the system to incident light, while  $M_{12}$ ,  $M_{13}$ ,  $M_{21}$  and  $M_{31}$  are related to dichroism properties of the media<sup>[10,12]</sup>. For the chiral nature of glucose, we discuss these 4 matrix elements in detail and expand Eq. (3) into

$$M_{ij}(\rho, \phi) = \mu_s \int_0^{+\infty} \frac{1}{r^2} \exp(-\mu_t(z+r)) F_{ij} dz,$$

$$F_{12} = b(\theta) \cos(2\phi + 2\alpha_1)(\cos^2 \alpha + 1) \\ + [a(\theta) \cos(2\phi + 2\alpha_1) \cos(2\alpha_2) \\ - d(\theta) \sin(2\alpha_1 + 2\phi) \sin(2\alpha_2)](\cos^2 \alpha - 1)$$

$$F_{13}(\phi, \theta, \alpha_1, \alpha_2, \alpha) = F_{12}(\phi + \frac{\pi}{4}, \theta, \alpha_1, \alpha_2, \alpha),$$

$$F_{21} = 2b(\theta) \sin(2\phi) \sin(2\alpha_2) \cos \alpha \\ + a(\theta) \cos(2\phi)(\cos^2 \alpha - 1) \\ + b(\theta) \cos(2\alpha_2) \cos(2\phi)(1 + \cos^2 \alpha),$$

$$F_{31}(\phi, \theta, \alpha_1, \alpha_2, \alpha) = F_{21}(\phi - \frac{\pi}{4}, \theta, \alpha_1, \alpha_2, \alpha), \quad (4)$$

where  $a(\theta)$ ,  $b(\theta)$ ,  $e(\theta)$  are derived from Mie theory<sup>[10]</sup>.

To investigate relationship between glucose-induced optical rotation degree and glucose concentration, Mueller matrix elements with and without glucose are

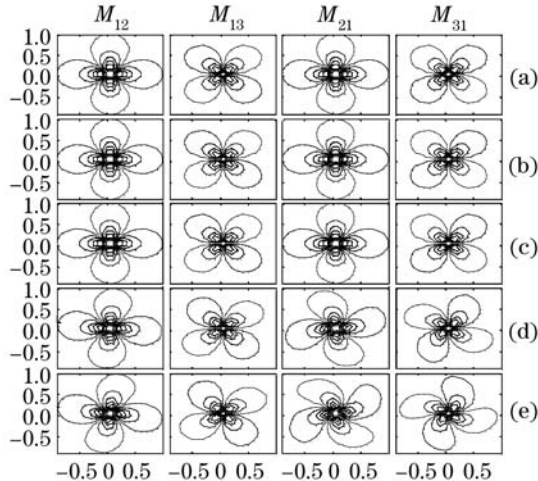


Fig. 2. Backscattered Mueller matrix patterns for  $M_{12}$ ,  $M_{13}$ ,  $M_{21}$ ,  $M_{31}$  matrix elements. Image size is  $10 \times 10$  (cm). (a)  $c_g = 0$  mg/dL; (b)  $c_g = 30$  mg/dL; (c)  $c_g = 60$  mg/dL; (d)  $c_g = 3 \times 10^5$  mg/dL; (e)  $c_g = 6 \times 10^5$  mg/dL.

subtracted and the results are integrated over radial axis  $r$

$$q_{ij}^{c_{gi}}(\phi) = \frac{1}{r_{\max}} \int_0^{r_{\max}} (M_{ij}^{c_{gi}} - M_{ij}^{c_{g0}}) dr, \quad (5)$$

where  $i, j$  are the same as Eq. (4),  $c_{gi}$  stands for glucose concentration.

Based on Eq. (4), Mueller matrix patterns for intralipid phantom at various glucose concentrations are calculated. Sphere diameter is set as 97 nm, refractive index of scatters and media are 1.57 and 1.33, respectively<sup>[6]</sup>; optical parameters are  $\mu_t = 1.01 \text{ cm}^{-1}$ ,  $\mu_s = 1.00 \text{ cm}^{-1}$ ; optical rotation coefficient  $k = 5.27 \text{ deg} \cdot \text{mL}/(\text{cm} \cdot \text{g})$ <sup>[13]</sup>. Figure 2 shows profiles of  $M_{12}$ ,  $M_{13}$ ,  $M_{21}$  and  $M_{31}$  for glucose concentration varying from 0 to  $6 \times 10^5$  mg/dL. Some of the figures are omitted for concision. It is found that the glucose in turbid media causes phase shift in the azimuthal orientation, but the rotation is only obvious in the case of high glucose concentrations which go far beyond the physiological range.

Figure 3 is obtained by introducing Eq. (5) into Fig. 2. Results of  $M_{13}$  and  $M_{31}$  are not shown because they have similar rules as  $M_{12}$  and  $M_{21}$ . The amplitude of the curves of  $q_{ij}^{c_{gi}}(\phi)$  increase as glucose concentration goes up. From Table 1 we can see that the amplitude is

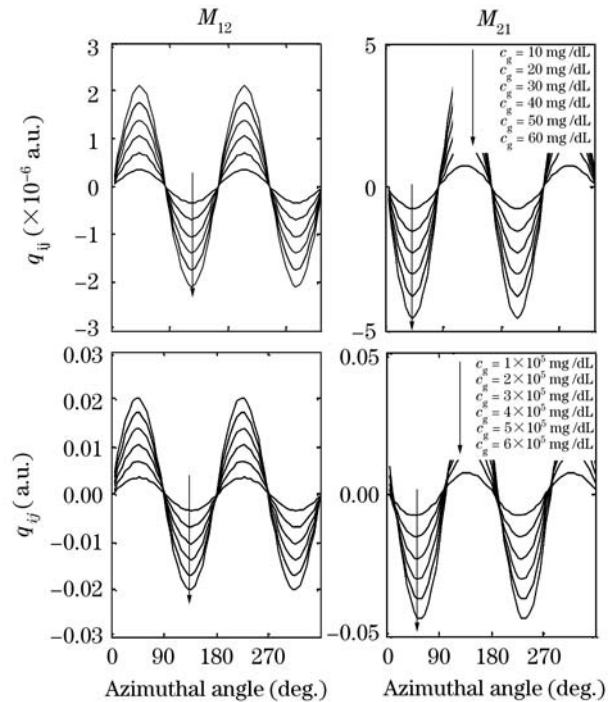


Fig. 3.  $q_{ij}^{c_g}(\phi)$  of  $M_{12}$ ,  $M_{21}$  matrix elements for different glucose concentrations.

Table 1. Amplitudes of  $q_{ij}^{c_g}(\phi)$  of  $M_{12}$ ,  $M_{21}$  for Different Glucose Concentrations

$c_g$ (mg/dL)	10	20	30	40	50	60
$M_{12}$ (a.u.)	$3.63 \times 10^{-7}$	$7.26 \times 10^{-7}$	$1.09 \times 10^{-6}$	$1.45 \times 10^{-6}$	$1.81 \times 10^{-6}$	$2.12 \times 10^{-6}$
$M_{21}$ (a.u.)	$7.73 \times 10^{-7}$	$1.55 \times 10^{-6}$	$2.32 \times 10^{-6}$	$3.09 \times 10^{-6}$	$3.87 \times 10^{-6}$	$4.64 \times 10^{-6}$
$c_g$ (mg/dL)	$1 \times 10^5$	$2 \times 10^5$	$3 \times 10^5$	$4 \times 10^5$	$5 \times 10^5$	$6 \times 10^5$
$M_{12}$ (a.u.)	$3.63 \times 10^{-3}$	$7.23 \times 10^{-3}$	$1.08 \times 10^{-2}$	$1.43 \times 10^{-2}$	$1.77 \times 10^{-2}$	$2.11 \times 10^{-2}$
$M_{21}$ (a.u.)	$7.71 \times 10^{-3}$	$1.53 \times 10^{-2}$	$2.26 \times 10^{-2}$	$2.96 \times 10^{-2}$	$3.61 \times 10^{-2}$	$4.2 \times 10^{-2}$

linear to the glucose concentration especially for the low concentration in the physiological range, hence optical rotation degree defined by  $q_{ij}^{c_g}(\phi)$  is nearly linear to the glucose concentration. This suggests possibility of using function  $q_{ij}^{c_g}(\phi)$  to compute glucose concentration and monitor glycemic status in diabetes patients.

Using single scattering model and Stokes-Mueller formalism, we derive expressions for backscattered Mueller matrix for  $M_{12}$ ,  $M_{13}$ ,  $M_{21}$  and  $M_{31}$  elements. Calculation results show that they present higher optical rotations as the concentration of glucose increases. Subtracting Mueller matrix elements with and without glucose and integrating the results over radial axis  $r$ , linear relationship between low glucose concentration in the physiological range and optical rotation degree defined by  $q_{ij}^{c_g}(\phi)$  can be obtained. Corresponding validate experiments are under preparation.

This work was supported in part by the National Natural Science Foundation of China (No. 60578056), the Program for New Century Excellent Talents in University by the Ministry of Education of China (No. NCET-04-0615), and the Governmental Education Bureau of Fujian Province (No. GB05339). H. Li is the author to whom the correspondence should be addressed, his e-mail address is hli@fjnu.edu.cn.

## References

1. J. Dillet, C. Baravian, F. Caton, and A. Parker, *Appl. Opt.* **45**, 4669 (2006).

2. M. Todorović, S. Jiao, L. V. Wang, and G. Stoica, *Opt. Lett.* **29**, 2402 (2004).
3. D. P. Cubián, J. L. A. Diego, and R. Rentmeesters, *Appl. Opt.* **44**, 358 (2005).
4. M. J. Raković, G. W. Kattawar, M. Mehrúbeoğlu, B. D. Cameron, L. V. Wang, S. Rastegar, and G. L. Coté, *Appl. Opt.* **38**, 3399 (1999).
5. S. Bartel and A. H. Hielscher, *Appl. Opt.* **39**, 1580 (2000).
6. A. H. Hielscher, J. R. Mourant, and I. J. Bigio, *Appl. Opt.* **36**, 125 (1997).
7. X. Wang, G. Yao, and L. V. Wang, *Appl. Opt.* **41**, 792 (2002).
8. S. Manhas, M. K. Swami, P. Buddhiant, N. Ghosh, P. K. Gupta, and K. Singh, *Opt. Express* **14**, 190 (2006).
9. J. T. Bruulsema, J. E. Hayward, T. J. Farrell, M. S. Patterson, L. Heinemann, M. Berger, T. Koschinsky, J. Sandahl-Christiansen, H. Orskov, M. Essenpreis, G. Schmelzeisen-Redeker, and D. Böcker, *Opt. Lett.* **22**, 190 (1997).
10. C. F. Bolden and D. R. Huffman, *Absorption and Scattering of Light by Small Particles* (Wiley, New York, 1983).
11. S. Wang, L. Xu, H. Li, and S. Xie, *Proc. SPIE* **5630**, 823 (2005).
12. W. S. Bickel and W. M. Bailey, *Am. J. Phys.* **53**, 468 (1985).
13. D. R. Lide, (ed.) *CRC Handbook of Chemistry and Physics* (81st edn., CRC Press, Boca Raton, 2000).